ELSEVIER

www.elsevier.nl/locate/jorganchem

Journal of Organometallic Chemistry 619 (2001) 299–304

Journal of Organometallic Chemistry

Structural and spectroscopic characterization of ruthenium(II) complexes with methyl, formyl, and acetyl groups as model species in multi-step CO_2 reduction

Dai Ooyama [a], Takashi Tomon [b], Kiyoshi Tsuge [b], Koji Tanaka [b,*]

[a] *Faculty of Education, Fukushima University, Kanayagawa, Fukushima 960-1296, Japan*
[b] *Department of Structural Molecular Science, Graduate University for Advanced Studies, Institute for Molecular Science, Myodaiji, Okazaki 444-8585, Japan*

Received 10 July 2000; received in revised form 18 September 2000; accepted 22 September 2000

Abstract

The molecular structures of Ru(II) complexes with methyl, formyl, and acetyl groups $[Ru(bpy)_2(CO)L]^+$ ($L = CH_3$, C(O)H and $C(O)CH_3$) were examined from the view point of active species in multi-step reduction of CO_2 on Ru. The methyl complex was prepared by the reaction of $[Ru(bpy)_2(OH_2)_2]^{2+}$ with trimethylsilyl acetylene and fully characterized by infrared, Raman, ^{13}C-NMR and single-crystal X-ray crystallography. Disorder of the Ru–CO and Ru–C(O)H bonds in the crystal structure of the formyl complex made it difficult to determine the bond parameters of the two groups accurately, but the molecular structure of the analogous acetyl complex, which was obtained by the reaction of $[Ru(bpy)_2(CO_3)]$ with propiolic acid, was determined by X-ray analysis. The ruthenium–carbonyl (Ru–C–O) bond angles of the methyl and acetyl complex with 174(1) and 175.5(5)°, respectively, are in the ranges of those of previously characterized $[Ru(bpy)_2(CO)L]^{n+}$ ($L = CO_2$, C(O)OH, CO and CH_2OH). On the other hand, the Ru–CH_3 and Ru–$C(O)CH_3$ bond distances showed unusual relationship against the stretching frequency in the Raman spectra.

Keywords: Ruthenium; X-ray crystallography; Methyl complex; Formyl complex; Acetyl complex; IR and Raman spectroscopy

1. Introduction

Much attention has been paid to the reduction of CO_2 aimed at synthesis of fuels and chemicals to cope with an increase in the concentration in the air and the oil shortage in the predictable near future [1]. Highly reduced products such as CH_4, C_2H_4, etc. were obtained in the electrochemical reduction of CO_2 on a Cu electrode in H_2O, though the binding mode of CO_2 on the surface of Cu plates still remained unclear [2]. Carbon dioxide bonded to metals with η^1-mode is smoothly converted to M–CO through M–C(O)OH under protic conditions [3], and three complexes, $[Ru(bpy)_2(CO)L]^{n+}$ (bpy = 2,2′-bipyridine; $L = CO_2$, C(O)OH, CO: $n = 0$, 1, 2) were well characterized [4]. Electro- and photochemical reduction of CO_2 catalyzed by metal complexes also has been extensively studied. Most of the reduction products in those homogeneous reactions are limited to CO and/or HCOOH [1,5]. On the other hand, some cationic metal–carbonyl complexes are successively reduced to methyl derivatives through formyl and hydroxymethyl ones [6]. Scheme 1, therefore, is a feasible pathway to CH_4 formation in the multi-step reduction of CO_2 catalyzed by metal complexes.

In fact, CH_3OH was produced in electrochemical reduction of CO_2 catalyzed by $[Ru(bpy)(trpy)(CO)]^{2+}$ (trpy = 2,2′:6′,2″-terpyridine) in EtOH–H_2O conducted at −20°C where thermally labile Ru–C(O)H is believed to play the key intermediate in the stepwise reduction from Ru–CO_2 to Ru–CH_2OH, but not to Ru–CH_3 (Scheme 1) [7]. The molecular structures of $[Ru(bpy)_2(CO)(C(O)H)]^+$ and $[Ru(bpy)_2(CO)(CH_3)]^+$ are, therefore, particularly interesting, because the crystal structures of $[Ru(bpy)_2(CO)L]^{n+}$ ($L = CO_2$, C(O)OH, CO, CH_2OH) were elucidated so far. It has

* Corresponding author.

0022-328X/01/$ - see front matter
PII: S0022-328X(00)00705-1

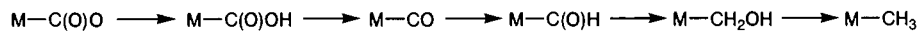

Scheme 1.

been shown that thermally labile $[Ru(bpy)_2(CO)(C(O)H)]^+$ easily disproportionates to $[Ru(bpy)_2(CO)_2]^{2+}$ and $[Ru(bpy)_2(CO)(CH_2OH)]^+$ in solutions, and reduction of $[Ru(bpy)_2(CO)(CH_2OH)]^+$ results in the Ru–CH_2OH bond cleavage without producing $[Ru(bpy)_2(CO)(CH_3)]^+$. Taking into account the importance of full characterization of the series of metal complexes in Scheme 1, the elucidation of the molecular structures of $[Ru(bpy)_2(CO)(C(O)H)]^+$ and $[Ru(bpy)_2(CO)(CH_3)]^+$ is expected to give fundamental information about the multi-step reduction of CO_2 on metals. Recently, $[Ru(bpy)_2(CO)(CH_3)]^+$was prepared through $[Ru(bpy)_2(OH_2)_2]^{2+}$ [8], though the reaction is not involved in Scheme 1. This work undertakes to elucidate the molecular structures of $[Ru(bpy)_2(CO)(CH_3)]^+$ and $[Ru(bpy)_2(CO)(C(O)H)]^+$ together with $[Ru(bpy)_2(CO)(C(O)CH_3)]^+$ as a model compound of the latter, and spectroscopic comparisons of these complexes.

2. Experimental

2.1. Materials and physical measurements

CH_3CN for electrochemical experiments was distilled over calcium hydride under nitrogen prior to use. Other chemicals were obtained as reagent grade. $[Ru(bpy)_2(CO)_2](PF_6)_2$ and $[Ru(bpy)_2(CO_3)]$ were prepared according to the literature methods [7,9]. Elemental analyses were performed at the Chemical Materials Center of the Institute for Molecular Science. IR spectra were recorded on a Shimadzu FTIR-8100 spectrometer using a KBr disk. ^{1}H- and ^{13}C-NMR were obtained on a JEOL EX270 spectrometer. Electronic spectra were acquired on a Shimadzu UV240 spectrophotometer. Raman spectra were measured on a Perkin–Elmer FT-Raman 2000 equipped with a Nd:YAG laser 1064 nm. All measurements were carried out in CH_3CN (ca. 50 mmol dm^{-3}) in 10 mm diameter glass tubes. Cyclic voltammetry were measured under N_2 conditions with a three-electrode system and a Hokuto Denko HAB-151 potentiostat connected to a Riken Denshi Co. F-35C X-Y recorder. The working and counter electrodes were platinum, and Ag–$AgNO_3$ (0.01 M) was used as a reference electrode. All potentials are reported in volts versus SCE in CH_3CN containing 0.1 M TBAP as supporting electrolyte. The $E_{1/2}$ value of ferrocene used as a standard is 0.40 V versus SCE in CH_3CN under our solution conditions [10].

2.2. Preparation of $[Ru(bpy)_2(CO)(CH_3)]PF_6$ (1)

The complex was prepared by a modified literature method [8]. To an aqueous solution of $[Ru(bpy)_2(CO_3)]$ (200 mg/40 cm^3) was mixed with two equivalents of HPF_6 solution (60%), and then stirred for 1 h at room temperature. The solution pH was kept around 7 by an addition of an aqueous solution of NaOH. The residue was separated by filtration and the resultant solution was mixed with trimethylsilyl acetylene (0.8 cm^3), and then refluxed for 2 h. The solution color changed gradually from dark brown to dark red and then brick color materials deposited. After this mixture was allowed to stand in a refrigerator for 2 h, the brick product was collected by filtration, washed with cold water and diethyl ether, and then dried in vacuo. The crude product was purified by column chromatography using Al_2O_3 (eluent: CH_2Cl_2–CH_3CN, 1:1 v/v). The volume of the solution was reduced to ca. 5 cm^3 using a rotary evaporator. The orange crystals were precipitated by the addition of diethyl ether, collected, and then washed with diethyl ether, and finally dried in vacuo. Yield 140 mg (53%). Anal. Found: C, 43.72; H, 3.18; N, 9.31. Calc. for $C_{22}H_{19}N_4OPF_6Ru$: C, 43.93; H, 3.19; N, 9.32%. IR spectrum (KBr): 1921 cm^{-1} (νC≡O), ^{1}H-NMR (δ, CD_2Cl_2): −0.05 (3H, CH_3), 7.25–9.16 (16H, bpy); ^{13}C-NMR (δ, CD_2Cl_2): −5.93 (CH_3), 123.09–158.15 (bpy), 203.97 (C≡O). Electronic spectrum: λ_{max}/nm (ϵ/M^{-1} cm^{-1}) 480 (3400), 356 (6700) in CH_3CN. CV: $E_{1/2} = -1.49$, −1.70 V, $E_{pa} =$ 1.06 V. Deuterium-substituted complex, $[Ru(bpy)_2(CO)(CD_3)]PF_6$, was prepared by the reaction in D_2O solution instead of H_2O.

2.3. Preparation of $[Ru(bpy)_2(CO)(C(O)H)]PF_6$ (2)

A colorless CH_3OH–$(CH_3)_2CO$ solution (3 cm^3, 2:1 v/v) of $[Ru(bpy)_2(CO)_2](PF_6)_2$ (10 mg) rapidly changed to yellow in color by an addition of aqueous $NaBH_4$ (1.5 equivalents) at −20°C. Then, diethyl ether (5 cm^3) was added into the solution at the temperature. Yellow single crystals of **2** gradually appeared out of the solution when the solution was allowed to stand at the temperature. Yield 5 mg (62%), ν(C≡O) 1952 cm^{-1} and ν(C=O) 1609 cm^{-1}. This complex was stable in the solid state though it slowly decomposes above −20°C in solution [11].

Table 1
Crystallographic data for $[Ru(bpy)_2(CO)(CH_3)]PF_6$ (**1**), $[Ru(bpy)_2(CO)(C(O)H)]PF_6$ (**2**), and $[Ru(bpy)_2(CO)(C(O)CH_3)]PF_6$ (**3**)[b]

	1	**2**	**3**
Chemical formula	$C_{22}H_{19}N_4ORuPF_6$	$C_{22}H_{17}N_4O_2RuPF_6$	$C_{23}H_{19}N_4O_2RuPF_6$
Formula weight	601.45	615.43	629.47
Temperature (K)	296	243	296
Crystal system	Orthorhombic	Orthorhombic	Orthorhombic
Space group	$P2_12_12_1$ (No. 19)	$P2_12_12_1$ (No. 19)	$Pbca$ (No. 61)
Unit cell parameters			
a (Å)	10.9739(6)	10.7046(4)	14.889(4)
b (Å)	12.4495(8)	12.6028(5)	24.408(4)
c (Å)	17.562(1)	17.4583(6)	13.490(5)
V (Å^3)	2399.4(2)	2355.3(1)	4902(2)
Z	4	4	8
No. of reflections measured	18856	18537	6239
No. of observations	1763 ($I>2\sigma(I_o)$)	2504 ($I>2\sigma(I_o)$)	3287 ($I>2.5\sigma(I_o)$)
Refinement method	Full-matrix least-squares on F		
Parameters	286	293	334
R[a]	0.062	0.048	0.047
R_w[b]	0.045	0.037	0.039

[a] $R = \Sigma \| F_o | - | F_c \| / \Sigma | F_o |$.
[b] $R_w = \{\Sigma_w(| F_o | - | F_c |)^2 / \Sigma_w F_o^2\}^{1/2}$.

2.4. Preparation of $[Ru(bpy)_2(CO)(C(O)CH_3)]PF_6$ (3)

The complex was also prepared by a modified literature method [8]. To an aqueous solution of $[Ru(bpy)_2(CO_3)]$ (200 mg/30 cm^3) was mixed with 0.5 cm^3 of propiolic acid, and then refluxed for 2 h. The solution color immediately changed from dark purple to yellow. Saturated aqueous KPF_6 solution was added and this mixture was stored in a refrigerator for 2 h. The yellow crystals were collected by filtration, washed with cold water and diethyl ether, and then dried in vacuo. The crude product was purified by column chromatography (Al_2O_3: CH_2Cl_2–CH_3CN, 2:1 v/v). Yield 184 mg (73%). Anal. Found: C, 43.76; H, 3.00; N, 9.01. Calc. for $C_{23}H_{19}N_4O_2PF_6Ru$: C, 43.89; H, 3.04; N, 8.90%. IR spectrum (KBr): 1939 cm^{-1} (νC≡O), 1607 cm^{-1} (νC=O), ^{1}H-NMR (δ, CD_2Cl_2): 2.21 (3H, CH_3), 7.34–9.47 (16H, bpy); ^{13}C-NMR (δ, CD_2Cl_2): 44.03 (CH_3), 122.91–156.96 (bpy), 202.61 (C≡O), 263.27 (C=O). Electronic spectrum: λ_{max}/nm (ϵ/M^{-1} cm^{-1}) 422 (2400), 334(sh) (5800) in CH_3CN. CV: $E_{1/2} = -1.38$, -1.61 V, $E_{pa} = 0.99$ V.

2.5. X-ray structure analyses

The single crystals of the complexes were obtained from CH_3CN–H_2O (**1**) or CH_3CN–ether mixtures (**3**). The single crystals of **2** were obtained as described in Section 2.3. An orange prismatic crystal of **1**, a yellow cubic crystal of **2**, and an yellow rhombic one of **3** having dimensions of $0.25 \times 0.10 \times 0.08$ mm (for **1**), $0.20 \times 0.30 \times 0.15$ mm (for **2**), and $0.25 \times 0.25 \times 0.25$ mm (for **3**), respectively, were mounted on glass fiber with epoxy resin. Data for **1** and **2** were collected by the ω scan technique with a Bruker Smart CCD diffractometer with the use of graphite monochromated Mo–K_α radiation ($\lambda = 0.71069$ Å) up to a 2θ maximum of 55°. Cell parameters were retrieved using SMART software and refined using SAINT on all observed reflections. Data reduction was performed with SAINT software which corrects for Lorentz polarization and decay. Absorption corrections were applied using SADABS. Data for **3** were collected by ω–2θ scan technique with a Rigaku AFC-5S diffractometer with the use of graphite monochromated Mo–K_α radiation ($\lambda =$ 0.71069 Å) up to a 2ϑ maximum of 55°. After corrections for Lorentz and polarization effects, absorption corrections from ψ scans were applied. All the calculation were carried out on an SGI indigo computer system using TEXSAN [12]. The structures were solved by direct methods (for **1** and **2**) or heavy-atom Patterson methods (for **3**) and expanded using Fourier techniques. The non-hydrogen atoms other than F atoms (for **1**) or O, F, and P atoms (for **2**) were refined anisotropically and hydrogen atoms were located by calculation and not refined. The oxygen atoms of the CO and C(O)H groups in **2** were completely disordered at two sites. Thus, the least-squares calculation including the disordered oxygen atoms and the structure was successfully refined. Crystallographic data are listed in Table 1 and selected bond distances and angles are listed in Table 2.

3. Results and discussion

Several attempts to prepare **1** by the reduction of $[Ru(bpy)_2(CO)(CH_2OH)]^+$ were unsuccessful due to se-

Table 2
Selected bond distances (Å) and angles (deg) for **1**, **2**, and **3**

	Bond distances		Bond Angles	
1	Ru1–C1	2.21(2)	Ru1–C2–O1	174(1)
	Ru1–C2	1.77(2)	C1–Ru1–C2	83.6(6)
	Ru1–N1	2.16(1)		
	Ru1–N2	2.057(8)		
	Ru1–N3	2.07(1)		
	Ru1–N4	2.031(9)		
	C2–O1	1.15(2)		
2	Ru1–C17	1.867(10)	Ru1–C17–O1	167(1)
	Ru1–C18	1.890(8)	Ru1–C17–O2	137.1(10)
	Ru1–N1	2.178(6)	Ru1–C18–O3	162.3(10)
	Ru1–N2	2.061(4)	Ru1–C18–O4	136(1)
	Ru1–N3	2.158(6)	C17–Ru1–C18	89.2(4)
	Ru1–N4	2.082(4)		
	C17–O1	1.08(1)		
	C17–O2	1.30(1)		
	C18–O3	1.16(1)		
	C18–O4	1.14(2)		
3	Ru–C1	2.038(5)	Ru–C3–O2	175.5(5)
	Ru–C3	1.836(6)	C1–Ru–C3	88.8(2)
	Ru–N1	2.070(4)	Ru–C1–O1	120.8(4)
	Ru–N2	2.137(4)	Ru–C1–C2	122.5(4)
	Ru–N3	2.190(4)	O1–C1–C2	116.7(5)
	Ru–N4	2.083(4)		
	C3–O2	1.153(6)		
	C1–O1	1.229(6)		
	C1–C2	1.478(8)		

lective cleavage of the Ru–CH_2OH bond prior to that of the $RuCH_2$–OH one. Accordingly, **1** was prepared by the reaction of $[Ru(bpy)_2(OH_2)_2]^{2+}$ with trimethylsilyl acetylene in H_2O. The orange methyl complex was soluble in CH_3CN, CH_2Cl_2, $(CH_3)_2CO$, and CH_3OH. The product prepared in D_2O unless otherwise under the same reaction conditions also satisfied the elemental analysis of the CH_3 complex and did not show the methyl signal in the ^{1}H-NMR spectra. Thus, methyl protons of **1** resulted from H_2O [13]. Based on the fact that $[Ru(bpy)(trpy)(C(O)H)]^+$ reacts with CO_2 to form $HCOO^-$ with generation of $[Ru(bpy)(trpy)(CO)]^{2+}$ (Scheme 2) [7], formyl complexes are considered to be the key intermediate affording either CH_3OH or HCOOH in the reduction of CO_2.

So we have successfully obtained single crystals of **2** in the reaction of $[Ru(bpy)_2(CO)_2](PF_6)_2$ with BH_4^- at -20°C. The X-ray analysis of the single crystals of **2** revealed the molecular structure of the complex with *cis*-orientation of the Ru–CO and Ru–C(O)H moieties. However, the bond distances and angles of the Ru–CO and Ru–C(O)H groups could not be determined due to disorder of the two groups in the crystal structure (Fig. 1). The ambiguity of the local structures due to disorder of the Ru–CO and Ru–C(O)H groups in the solid state was not improved in the X-ray measurement conducted even at -150°C. We, therefore, turned our attention to the molecular structure of **3** with a –$C(O)CH_3$ group in place of the –C(O)H moiety by considering that a small difference in the sizes between CO and C(O)H moieties causes the disorder of the two groups in the solid state of **2**. Complex **3** was prepared by the reaction of $[Ru(bpy)_2(CO_3)]$ with propiolic acid in H_2O. The yellow complex **3** was also soluble in some organic solvents described above.

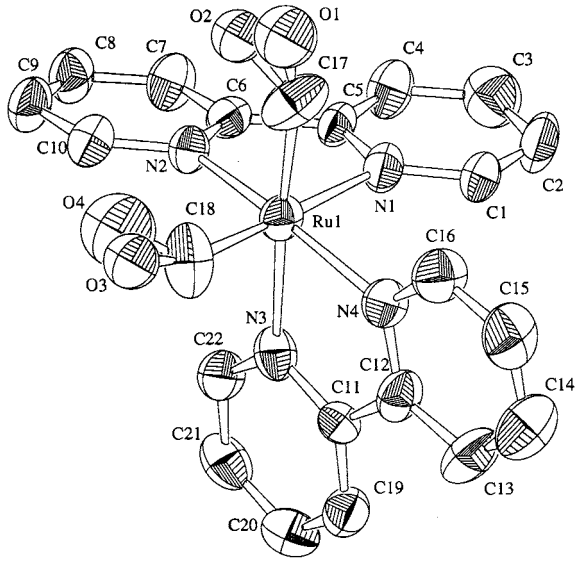

Fig. 1. Molecular structure of $[Ru(bpy)_2(CO)(C(O)H)]^+$ (**2**) with atom labeling. Hydrogen atoms are omitted for clarity. Oxygen atoms in CO and C(O)H groups are disordered.

Table 3
Summary of wavenumber and bond distance for **1** and **3**

	1	**3**
ν(C≡O) / cm^{-1}	1921	1939
ν(Ru–L) / cm^{-1}	529	511
d(Ru–L) / Å	2.21	2.04

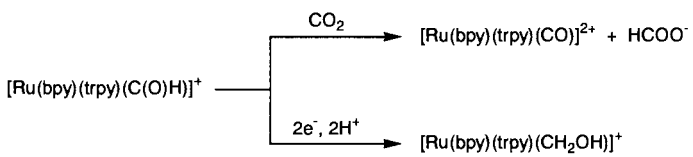

Scheme 2.

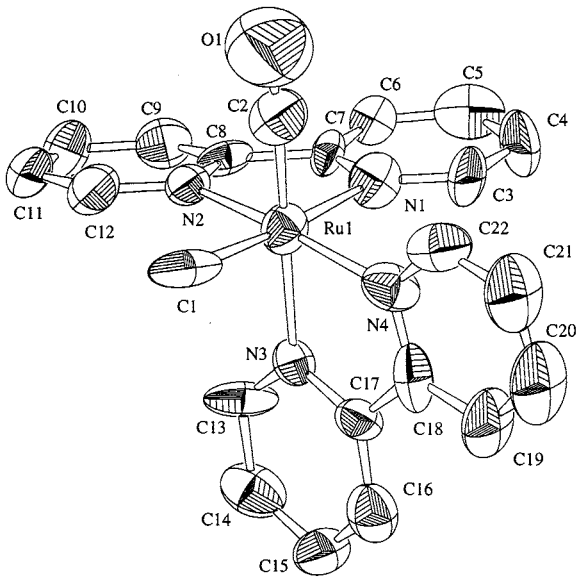

Fig. 2. Molecular structure of $[Ru(bpy)_2(CO)(CH_3)]^+$ (**1**) with atom labeling. Hydrogen atoms are omitted for clarity.

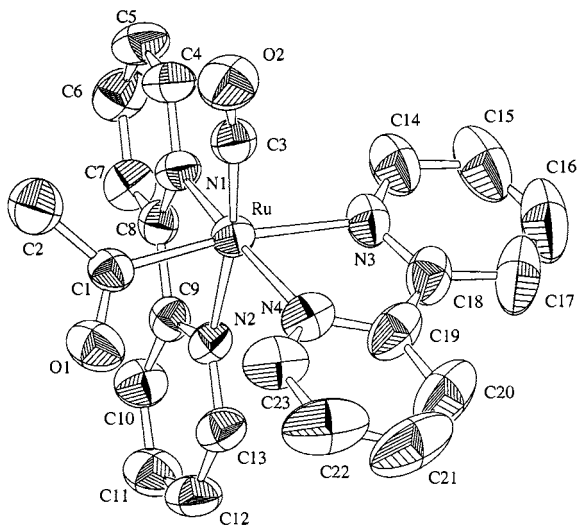

Fig. 3. Molecular structure of $[Ru(bpy)_2(CO)(C(O)CH_3)]^+$ (**3**) with atom labeling. Hydrogen atoms are omitted for clarity.

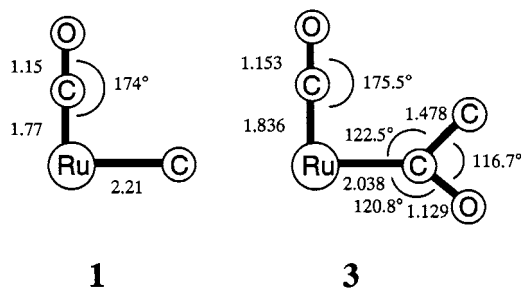

Fig. 4. Selected geometrical parameters of $Ru(CO)(CH_3)$ (**1**) and $Ru(CO)(C(O)CH_3)$ (**3**) moieties (Å, °).

Table 3 summarizes the $\nu(C{\equiv}O)$ and $\nu(Ru–L)$ bands ($L = CH_3$ (**1**) and $C(O)CH_3$ (**3**)) together with the distances between Ru and carbon bond in L. Complex **1** showed the $\nu(C{\equiv}O)$ band at 1921 cm^{-1}, which is close to that of $[Ru(bpy)_2(CO)(CH_2OH)]^+$ [7], suggesting that the electron donor ability of methyl group is comparable to that of CH_2OH group. The Raman spectra of **1** displayed a medium peak at 529 cm^{-1}, which shifted to 523 cm^{-1} in the CD_3 complex. Taking into account that metal–alkyl complexes usually show their $\nu(M–C)$ band in the range of 500 to 600 cm^{-1} [14], the 529 cm^{-1} band of **1** is reasonably assigned to the $\nu(Ru–CH_3)$ band. The IR spectrum of **3** showed the $\nu(C{\equiv}O)$ band at 1939 cm^{-1} and the $\nu(C{=}O)$ band at 1607 cm^{-1}, which are similar to those of $[Ru(bpy)_2(CO)(C(O)H)]^+$ (**2**) [11]. Thus, the electron donor ability of acetyl group is comparable to that of formyl group. The Raman spectra of **3** displayed a medium peak at 511 cm^{-1} which resides in the range 510–520 cm^{-1} of the $\nu(Ru–L)$ band of $[Ru(bpy)_2(CO)L]^{n+}$ ($L = CO_2$, C(O)OH, and $C(O)OCH_3$) [15]. The 511 cm^{-1} band of **3**, therefore, is attributable to the $\nu(Ru–C(O)CH_3)$ mode.

In the series of metal complexes in Scheme 1, the molecular structure of $[Ru(bpy)_2(CO)(C(O)H)]^+$ (**2**) was not determined due to the disorder between CO and C(O)H groups. The molecular structure of the formyl complex could be presumed by that of **3** from the similarity of the IR spectra. The crystal structures of **1** and **3** are depicted in Fig. 2 and Fig. 3, respectively. The both cations of **1** and **3** also have the expected octahedral coordination geometry. The two bidentate bpy ligands are situated in a *cis* position with each other, and the bond distances and angles of the bpy ligands are similar to those observed in the other complexes of this series. Accordingly, the structural differences in the present complexes are focused on the $Ru(CO)(CH_3)$ (for **1**) and $Ru(CO)(C(O)CH_3)$ (for **3**) moieties (Fig. 4). As shown in Fig. 4, the Ru–C–O bond angles are linear (174(1)° for **1** and 175.5(5)° for **3**) and the angles are within the ranges observed for other structurally characterized $[Ru(bpy)_2(CO)L]^{n+}$ complexes ($L = CO$, CO_2, C(O)OH, $C(O)OCH_3$, and CH_2OH) [4,7]. On the other hand, the bond distance between ruthenium and methyl carbon for **1** (2.21(2) Å) is the longest one in the series of $[Ru(bpy)_2(CO)L]^{n+}$, whereas the distance between ruthenium and acetyl carbon for **3** (2.038(5) Å) is the middle one [16]. Based on the fact that the Ru–C bond distance of $[Ru(bpy)_2(CO)_2]^{2+}$ is 1.89 Å (average) [4a], the Ru–C bond distance lengthens in the order of Ru–Csp < Ru–Csp^2 < Ru–Csp^3. Thus, the increase in the d_π-p_π interaction between Ru and carbon atoms shortens the Ru–C bond distance. The low wavenumber of the $\nu(C{\equiv}O)$ band of **1** is ascribed to strong electron donor character of sp^3 carbon to Ru compared with that of sp^2 and sp carbon. Moreover, Raman spectra of

$[Ru(bpy)_2(CO)L]^{n+}$ revealed that ν(Ru–Csp), ν(Ru–Csp^2), and ν(Ru–Csp^3) bands of the complexes reside in the range of 444 cm^{-1} (L = CO), 510–520 cm^{-1} (L = CO_2, C(O)OH, $C(O)OCH_3$, and $C(O)CH_3$), and 525–560 cm^{-1} (L = CH_3 and CH_2OH), respectively [15,16].

4. Supplementary material

Crystallographic data for the structural analyses have been deposited with the Cambridge Crystallographic Data Centre, CCDC Nos. 146459 for **1**, 146538 for **2**, and 146537 for **3**. Copies of this information may be obtained free of charge from The Director, CCDC, 12 Union Road, Cambridge CB2 1EZ, UK (Fax: +44-1223-336033; e-mail: deposit@ccdc.ac.uk or www: http://www.ccdc.cam.ac.uk).

Acknowledgements

The authors are grateful to Professor Makoto Fujita of Nagoya University for the use of X-ray diffractometer and to Ms. Emi Yokoyama of Fukushima University for her technical assistance. This work was supported by the Joint Studies Program (1999–2000) of the Institute for Molecular Science.

References

[1] (a) J. Costamagna, G. Ferraudi, J. Canales, J. Vergas, Coord. Chem. Rev. 148 (1996) 221. (b) D.H. Gibson, Chem. Rev. 96 (1996) 2063. (c) K. Tanaka, Bull. Chem. Soc. Jpn. 71 (1998) 17.
[2] (a) Y. Hori, A. Murata, R. Takahashi, S. Suzuki, J. Am. Chem. Soc. 109 (1987) 5022. (b) Y. Hori, A. Murata, R. Takahashi, S. Suzuki, J. Chem. Soc. Chem. Commun. (1988) 17.
[3] (a) K. Tanaka, M. Morimoto, T. Tanaka, Chem. Lett. (1983) 901. (b) H. Ishida, K. Tanaka, M. Morimoto, T. Tanaka, Organometallics 5 (1986) 724.
[4] (a) H. Tanaka, B.C. Tzeng, H. Nagao, S.M. Peng, K. Tanaka, Inorg. Chem. 32 (1993) 1508. (b) K. Toyohara, H. Nagao, T. Adachi, T. Yoshida, K. Tanaka, Chem. Lett. (1996) 27.
[5] (a) B.P. Sullivan, K. Krist, H.E. Guard (Eds.), Electrochemical and Electrocatalytic Reduction of Carbon Dioxide, Elsevier, Amsterdam, 1993. (b) M.M. Halmann (Ed.), Chemical Fixation of Carbon Dioxide, CRC Press, London, 1993. (c) K. Tanaka, Adv. Inorg. Chem. 43 (1995) 409.
[6] (a) P.M. Treichel, R.L. Schubhin, Inorg. Chem. 6 (1967) 1328. (b) C. Lapinte, D. Astruc, J. Chem. Soc. Chem. Commun. (1983) 430. (c) C. Lapinte, D. Catheline, D. Astruc, Organometallics 7 (1988) 1683.
[7] H. Nagao, T. Mizukawa, K. Tanaka, Inorg. Chem. 33 (1994) 3415.
[8] C. Mountassir, T.B. Hadda, H. Le Bozec, J. Organomet. Chem. 388 (1990) C13.
[9] E.C. Johnson, B.P. Sullivan, D.J. Salmon, S.A. Adeyemi, T.J. Meyer, Inorg. Chem. 17 (1978) 2211.
[10] N.G. Connelly, W.E. Geiger, Chem. Rev. 96 (1996) 877.
[11] K. Toyohara, H. Nagao, T. Mizukawa, K. Tanaka, Inorg. Chem. 34 (1995) 5399.
[12] TEXSAN: Single Crystal Structure Analysis Software, Version 1.6; Molecular Structure Corp., Woodlands, TX, 1993.
[13] C. Bianchini, J.A. Casares, M. Peruzzini, A. Romerosa, F. Zanobini, J. Am. Chem. Soc. 118 (1996) 4585.
[14] K. Nakamoto, Infrared and Raman Spectra of Inorganic and Coordination Compounds, 4th ed., Wiley, New York, 1986, pp. 375–377.
[15] G. Davidson (Ed.), Spectroscopic Properties of Inorganic and Organometallic Compounds, vol. 30, The Royal Society of Chemistry, London, 1997, pp. 290–295.
[16] K. Toyohara, K. Tsuge, K. Tanaka, Organometallics 14 (1995) 5099.